ISTITUTO NAZIONALE DI FISICA NUCLEARE
Laboratori Nazionali di Frascati

LNF-80/12(R)
10 Marzo 1980

R. Barbini and G. Vignola:

LELA: A FREE ELECTRON LASER EXPERIMENT IN ADONE.

Servizio Documentazione
dei Laboratori Nazionali di Frascati
Cas. Postale 13 - Frascati (Roma)

INFN - Laboratori Nazionali di Frascati
Servizio Documentazione

LNF-80/12(R)
10 Marzo 1980

R. Barbini(x) and G. Vignola(x) :

LELA : A FREE ELECTRON LASER EXPERIMENT IN ADONE.

1. - INTRODUCTION.

In the last few years there has been an increasing interest on the study of free electron lasers. The experiments performed by Madey and coworkers[1] with the Stanford Superconducting Linac showed that it is possible to achieve both amplification of the coherent radiation and laser oscillation[2] by sending an electron beam through the periodic field of a magnetic undulator.

Tunability over a wide wavelength range (0.1-20 μm), sharp linewidth ($\Delta\lambda/\lambda = 10^{-7} - 10^{-4}$) output power and efficiency make this type of laser an attractive tool for research in many fields such as photochemistry, molecular physics, solid state physics, etc.

Moreover, if by the aid of technical improvements the average output power could be raised to the kw level and the efficiency to some percent, then many industrial applications and probably laser isotope separation could benefit from this new kind of laser.

From the theoretical point of view various approaches have been attempted in studying the interaction between electrons and radiation field, viz: quantum and classical theories, single particle and many particles (Maxwell-Boltzmann) pictures.

While we refer, for more details, to the extensive review articles of C. Pellegrini[3,4] on this argument, we just recall here that all theoretical treatments lead to the experimentally verified small signal gain formula, while disagreements appear on other aspects of the FEL (large signal, saturation). In particular, since all experimental information comes from Madey's experiments only, the discussion is still open on which is the best electron accelerator to be used in connection with the FEL (storage ring, linac, microtron or else). However, the interaction between radiation and the recirculated e^- beam in a storage ring is, from the experimental point of view, an open problem worth of accurate investigation: we therefore propose to build a free electron laser device (LELA) by installing a suitable magnetic undulator on a straight section of the storage ring Adone.

(x) - On leave from CNEN - Centro di Frascati.

The main goals of the LELA experiment are to collect informations on:

- amplification of radiation with the aid of an external "seed" laser (Argon laser $\lambda = 5145$ Å);
- wavelength and optical gain as functions of electron energy and undulator magnetic field;
- transient behaviour of the laser radiation;
- steady-state interaction between laser radiation and stored electrons (i. e. optical gain vs. electron energy, maximum extractable optical power, optical spectrum).

2. - FEL AND STORAGE RING PARAMETERS.

It is proposed to install a transverse undulator on the Adone straight section no. 11. An optical cavity can then be built by adding a mirror at each end of the straight section, or an external laser beam can be sent along the s. s. axis to interact with the electron beam and the undulator field (see Fig. 8). A layout of the ring is shown in Fig. 1.

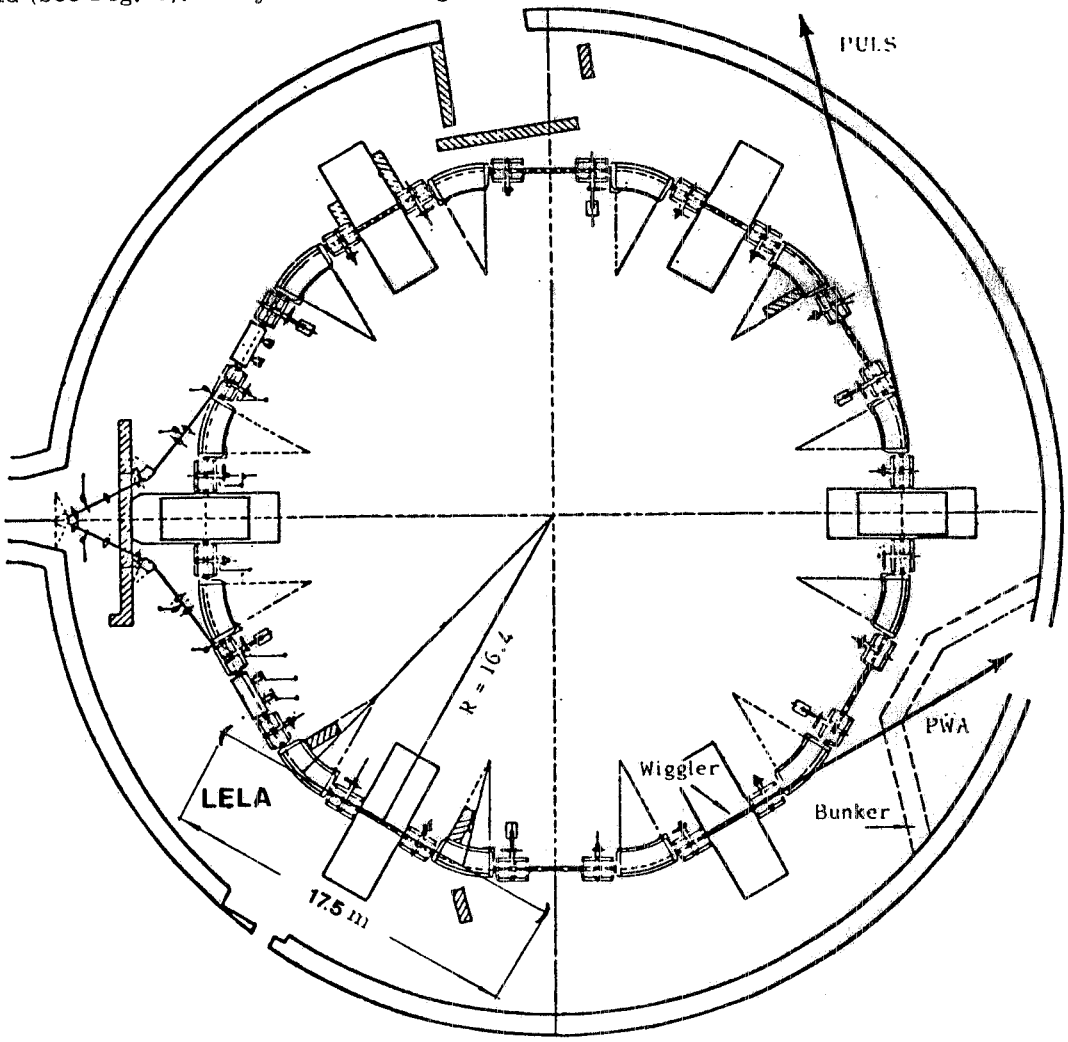

FIG. 1 - Layout of the LELA experiment in Adone.

In order to minimize the laser beam losses in the optical cavity (oscillator experiment) and to avoid head-on collisions between photons and electrons, it is convenient to operate Adone with three electron bunches and to adjust the optical cavity length to half the distance between two consecutive bunches: a single photon bunch will then travel inside the optical cavity and will meet one of the electron bunches once per every round trip.

The spontaneous radiation wavelength, observed on the undulator axis (≡ y axis) is given by (see Appendix A):

$$\lambda = \frac{\lambda_q}{2\gamma^2}(1 + K^2) \tag{1}$$

where λ_q is the undulator period and $\gamma = E/m_o c^2$.

For a pure cosine-like vertical magnetic field on axis

$$B_z = B_o \cos \frac{2\pi}{\lambda_q} y \tag{2}$$

the parameter K is given by

$$K = \frac{eB_o \lambda_q}{\sqrt{2}\, 2\pi m_o c^2} \simeq 6.6\, B_o(KG)\, \lambda_q(m)\ . \tag{3}$$

By defining the R. M. S. magnetic field on axis by

$$\bar{B} = \left[\frac{1}{\lambda_q}\int_0^{\lambda_q} |B_z(y)|^2\, dy\right]^{1/2} \tag{4}$$

one can also write

$$K = 9.33\, \bar{B}(KG)\, \lambda_q(m)\ . \tag{5}$$

According to eq. (1), the wavelength can be tuned by varying either the electron energy or the undulator magnetic field or both. In Fig. 2 the wavelength λ is plotted vs. electron energy E for $\lambda_q = 11.6$ cm and three values of the parameter K (K = 1, $\sqrt{2}$, 3.412).

In order to avoid all unnecessary technical complications, we choose to operate in the visible wavelength region with magnetic fields that can be achieved with standard magnet technology. The electron energy should be the highest possible in order to achieve the highest possible peak current.

The undulator period should be designed so as to accomodate the maximum number of periods in the fixed length of the Adone straight section ($\simeq$ 2.5 m). On the other hand the achievable magnetic field on axis will depend both on the undulator period and on the gap

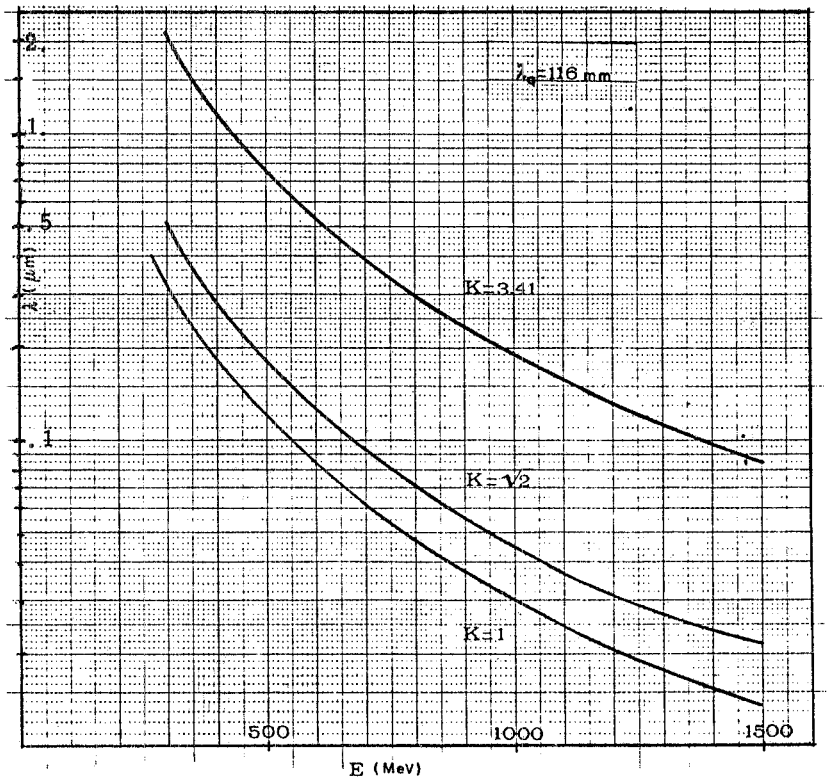

FIG. 2 - Optical wavelength vs. electron energy.

height[6,7]. Finally electron energy, undulator period and magnetic field are connected by the wavelength eq. (1). Taking into account the above constraints and using the results of magnetic field calculations[5,6] we end up with the basic FEL parameters listed in Tab. I.

TABLE I

Undulator period	λ_q = 11.6 cm
Number of periods	N = 20
Undulator length	L_w = 2.32 m
Homogeneous broadening	$\left[\frac{\Delta\lambda}{\lambda}\right]_o = \frac{\lambda_q}{2L_w}$ = 2.5 %
RMS magnetic field on axis	$\bar{B}$ = 3153 G K = 3.412
Electron energy	E = 610 MeV
Radiation wavelength	λ = 5145 Å
Optical cavity length	L = 17.5 m

The FEL gain has been demonstrated[8,1] to be inversely proportional to the square of the total spontaneous radiation linewidth, which, in turn, is made up of two contributions, homogeneous and inhomogeneous broadening, adding quadratically. We require the inhomogeneous broadening to contribute a negligible amount to the sum.

This places upper limits on the e-beam angular divergence and energy spread. It also requires that the off energy η function vanishes in the section where the undulator is mounted. By increasing the number of independent qdp families from 2 to 4, Adone can be made into a six-period machine with η vanishing in alternative straights. The standard cell is characterized by the following magnetic sequence:

$$\frac{0}{2},\ QD1,\ QF1,\ B,\ QD2,\ QF2,\ 0,\ QF2,\ QD2,\ B,\ QF1,\ QD1,\ \frac{0}{2},$$

and the resulting optical functions are shown in Figg. 3 and 4.

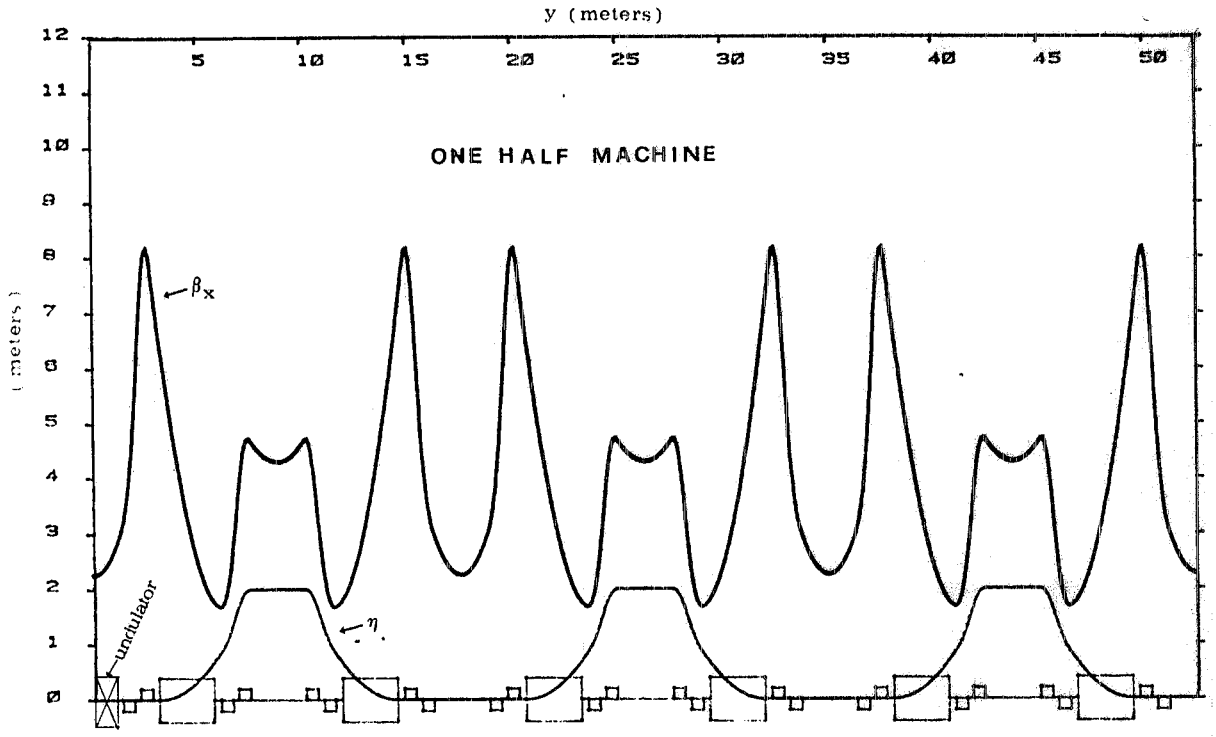

FIG. 3 - Radial betatron function β_x and off-energy function η for one half machine.

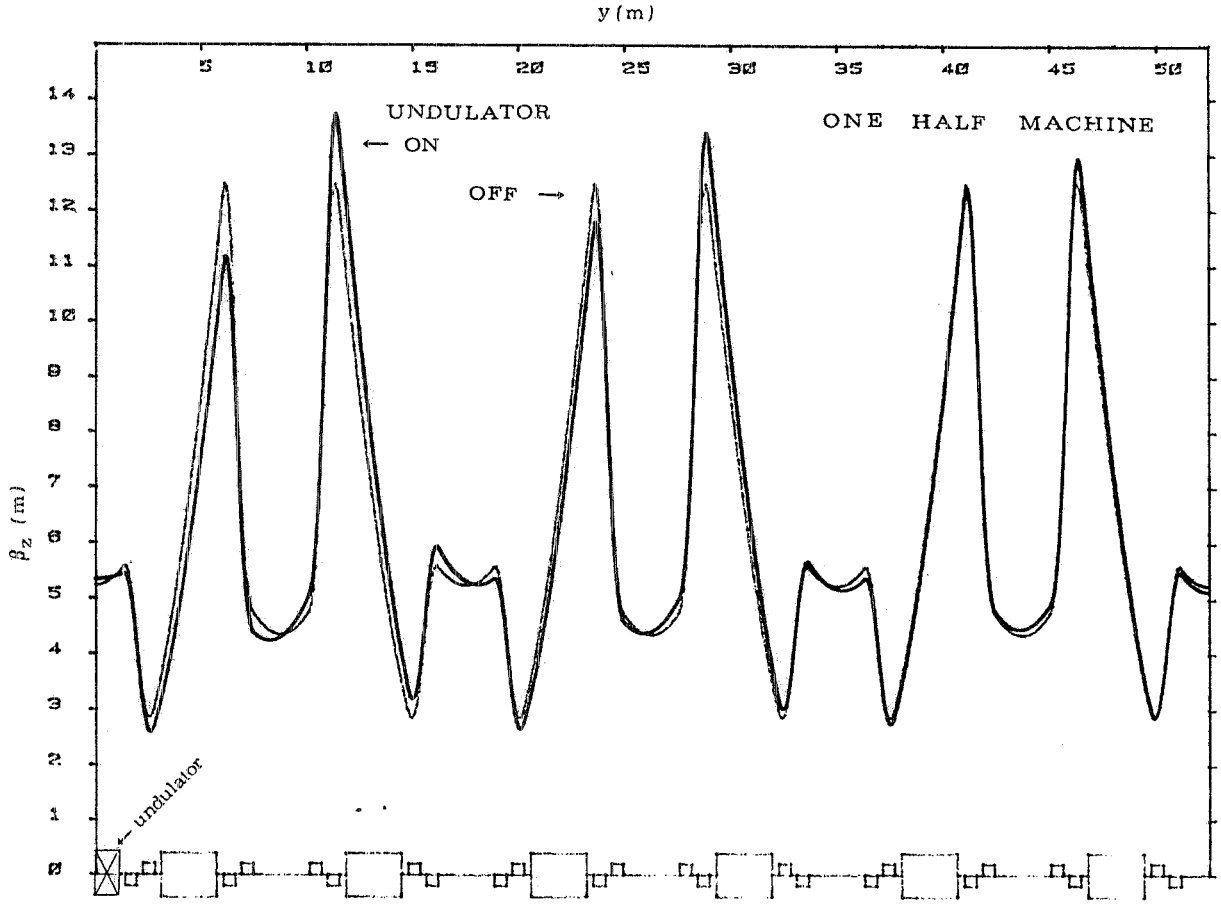

FIG. 4 - Vertical betatron function β_z for one half machine, with undulator on and off (in both cases $\nu_x = 5.15$ and $\nu_z = 3.15$).

The main machine parameters and the quadrupole strengths $G/B\varrho$ are listed in Table II and III, respectively. It is also assumed that the new 51.4 MHz RF cavity, at present under construction, will be installed and operating.

3. - SMALL SIGNAL GAIN AND BUNCH LENGTHENING.

The FEL small signal gain per pass in the homogeneous broadening regime and for a monochromatic e beam reads[4] (see also Appendix C):

$$g_o = -32\sqrt{2}\,\pi^2\,\lambda^{3/2}\,\lambda_q^{1/2}\,\frac{K^2}{(1+K^2)^{3/2}}\,\frac{I_p}{I_A}\,\frac{N^3}{\Sigma_L}\,f(x) \qquad (6)$$

where

$I_A = \frac{ec}{r_o} = 17.000$ A ,

I_p = peak current/bunch ,

$x = 4\pi N\,\frac{\gamma_o - \gamma_R}{\gamma_R}$,

γ_o = working energy (in unit of $m_o c^2$),

γ_R = resonance energy $= \left[\frac{\lambda_q}{2\lambda}(1+K^2)\right]^{1/2}$,

$f(x) = -\frac{1}{x^3}\left\{\cos x - 1 + \frac{1}{2}x\sin x\right\}$.

TABLE II

Electron energy		$E = 610$ MeV
Momentum compaction		$\alpha_c = 1.36 \times 10^{-2}$
Fractional energy spread		$\sigma_p = 2.3 \times 10^{-4}$
Invariant		$\langle H \rangle = 0.38$ m
Radial emittance (off coupling)		$A_x = 0.25$ mm x mrad
Energy loss in bending magnets		$U_o = 2.45$ keV/turn
Energy loss in undulator		$U_w = 109$ eV/pass
Radial betatron tune		$\nu_x = 5.15$
Vertical betatron tune		$\nu_z = 3.15$
Radial natural chromaticity		$C_x = -1.06$
Vertical natural chromaticity		$C_z = -1.61$
Damping partition numbers		$J_s = 2$; $J_x = J_z = 1$
Damping times		$\tau_i = 174/J_i$ msec
Revolution frequency		$f_o = 2.856$ MHz
RF frequency		$f_{RF} = 51.4$ MHz
Harmonic number		$h = 18$
Number of bunches		$n_b = 3$
1 RF cavity :	RF peak voltage	$V_{RF} = 300$ kV
	RF acceptance	$\varepsilon_{RF} = 3.58\%$
2 RF cavities :	RF peak voltage	$V_{RF} = 600$ kV
	RF acceptance	$\varepsilon_{RF} = 5.06\%$

TABLE III

Element	$\nu_x = 5.15$, $\nu_z = 3.15$ G/Bϱ (m^{-2})	$\nu_x = 5.15$, $\nu_z = 3.15$ G/Bϱ (m^{-2})
undulator(x)	0	- 0.0240
QD 1	- 0.8542	- 0.8426
QF 1	1.2761	1.2706
QD 2	- 1.1692	- 1.1692
QF 2	1.1325	1.1325

(x) for the undulator's transfer matrix see Appendix A.

The function f(x) is plotted in Fig. 5 and is proportional to the derivative of the spontaneous emission lineshape $(\frac{\sin x/2}{x/2})^2$ (homogeneously broadened). By assuming its maximum value (= - 0.0675 for x = 2.6056) and taking for the E. M. beam cross section the value $\bar{\Sigma}_L \frac{L_w \lambda}{\sqrt{3}}$ (see eq. (26)), together with the parameters listed in Table I, the gain g_o can be written

$$g_o = 6.7 \times 10^{-4} \, I_p(A) \cong 3 \times 10^{-3} \frac{i\,(mA)}{\sigma_y\,(cm)} \tag{7}$$

where $I_p(A)$ is the peak current/bunch ($I_p = c/2\ 35\ \sigma_y f_o$), i(mA) is the mean current/bunch and σ_y is the R. M. S. bunch length.

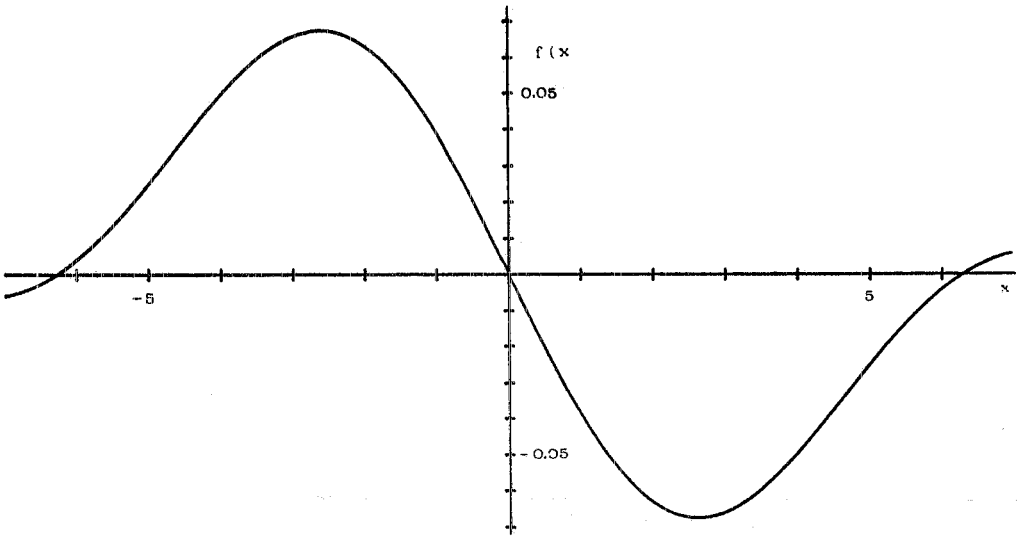

FIG. 5 - The gain function.

For the radiation build-up to take place, the optical gain per pass must exceed the cavity losses. Diffraction losses are negligible (see below) while mirror absorption and transmissivity can reasonably be kept below a total of 4‰. We require, by consequence, that the gain be raised to the level of percent, which can be accomplished with mean currents of some tens mA/bunch and σ_y of the order of cm (see (7)): at our working energy (610 MeV) the anomalous bunch lengthening phenomenon must therefore be properly taken in account.

Both according to the anomalous lenghtening model of Chao-Gareyte[9] and to the experimental results obtained in Adone[10], σ_y can be written as

$$\sigma_y(cm) \cong 1.84 \, R_{(m)}^{3/2.68} \, \xi_{(mA/keV)}^{1/2.68} \tag{8}$$

where R = 16.72 m is the mean radius of the machine and ξ is given by

$$\xi = \frac{i \alpha_c}{\nu_s^2 E} \tag{9}$$

with

$\nu_s = \Omega_s / \omega_o$,

Ω_s = angular frequency of the energy oscillations,

ω_o = angular frequency of revolution

By defining

$$m = \nu_s / \alpha_c$$

and with $\alpha_c = 1.36 \times 10^{-2}$ (see Table II) equation (8) becomes

$$\sigma_y\,(\text{cm}) = 16.26 \left[\frac{i\,(\text{mA})}{m^2\,E\,(\text{MeV})} \right]^{1/2.68} . \tag{10}$$

By inserting eq. (10) into (7) we have :

$$g_o = 1.83 \times 10^{-4}\; m^{2/2.68}\; i_{(\text{mA})}^{1.68/2.68}\; E_{(\text{MeV})}^{1/2.68} \tag{11}$$

We just recall here that the parameter m can be written[11] as

$$m = \left[\frac{h\,e\,V_{RF}}{2\pi\,\alpha_c\,E} \right]^{1/2} \tag{12}$$

while the RF acceptance for energy oscillation is ($V_{RF} \gg U_o/c$)

$$\varepsilon_{RF} \simeq \frac{2}{h}\, m \ . \tag{13}$$

In Fig. 6 we plot the R. M. S. bunch length σ_y vs. bunch current both with and without anomalous lengthening, and for the two cases V_{RF} = 300 KV and V_{RF} = 600 KV. Accordingly, Fig. 7a and 7b show the corresponding gain curves.

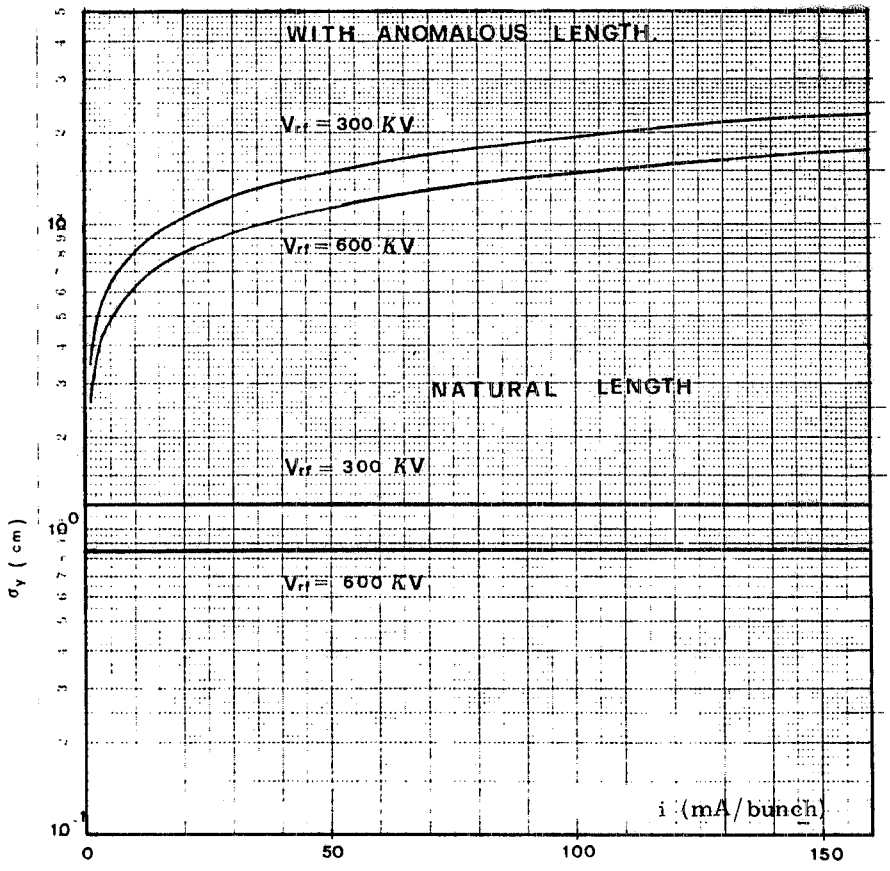

FIG. 6 - Natural and anomalous bunch length σ_y for V_{RF} = 300 KV and V_{RF} = 600 KV.

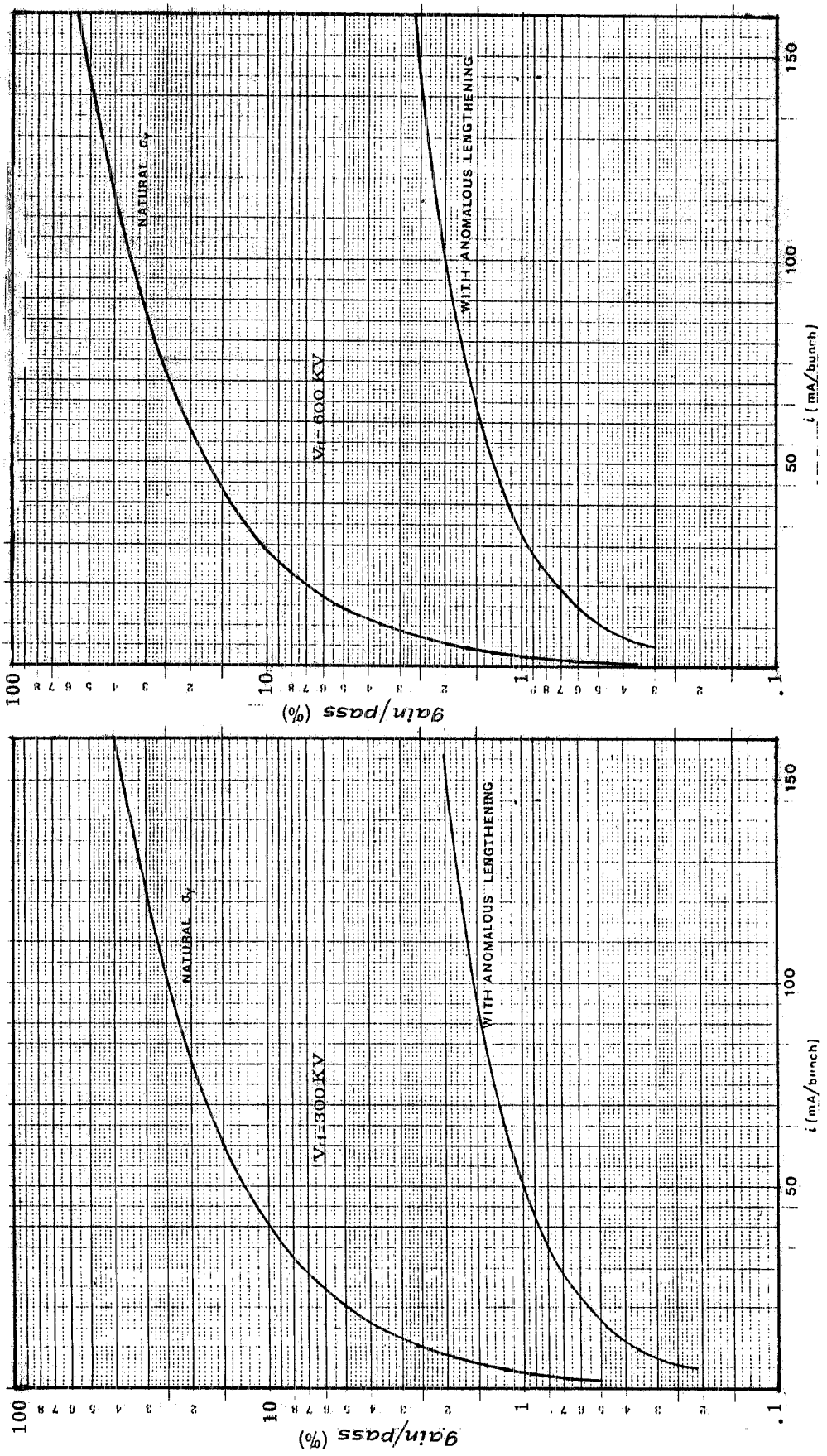

FIG. 7 - Optical gain/pass vs. mean current/bunch. a) V_{RF} = 300 KV , b) V_{RF} = 600 KV.

We conclude that the anomalous lengthening significantly affects the gain. Accurate measurements at the energy and currents considered, with the new RF system, will have to be performed. Our present thinking is that the Chao-Gareyte type extrapolation gives an upper limit to the anomalous lenthening and, consequently, a lower limit to the gain.

4. - ELECTRON BEAM LIFETIMES.

E-beam lifetimes are evaluated by taking into account the single and multiple Touschek effect, the vacuum chamber aperture and the RF acceptance.

4. 1. - Touschek effect.

By using a computer code developed by Wang[18] we obtained, for i = 50 mA/bunch, the Touschek lifetimes τ_T (including multiple Coulomb scattering) and the beam cross section enlargement ratios ζ listed in Table IV (see also ref. (13)).

TABLE IV

	V_{RF} = 300 KV		V_{RF} = 600 KV	
	τ_T(hours)	ζ	τ_T(hours)	ζ
Without anomalous lengthening	22.9	2.05	48.2	2.24
With anomalous lengthening	449	1.08	1056	1.10

4. 2. - Vacuum chamber aperture.

We recall[11] that the total radial spread can be written as

$$\sigma_x^2 = \sigma_{x\beta}^2 + \sigma_{x\varepsilon}^2 \quad , \tag{14}$$

where

$$\sigma_{x\beta}^2 = \sigma_p^2 \langle H \rangle_{mag} \frac{J_s}{J_x} \beta_x \frac{1}{1+\chi^2} \tag{15}$$

is the betatron contribution (χ^2 is the coupling coefficient for betatron oscillations) and $\sigma_{x\varepsilon}^2$ is the energy spread contribution.

Though nothing can be said on the transient laser behaviour, we can reasonably take that if a steady state is to be reached, then the R. M. S. electron energy spread should attain the equilibrium value

$$\frac{2\Delta\gamma}{\gamma} = \frac{1}{2N} \quad , \tag{16}$$

so that

$$\sigma_{x\varepsilon} \approx \eta \frac{\Delta\gamma}{\gamma} \approx \eta \frac{1}{4N} \quad , \tag{17}$$

which would be the major contribution to the total spread (14), occurring wherever $\eta \neq 0$.

In this case the beam lifetime is[12]

$$\tau_{qx} = \tau_x \, e^{(d/\sigma_{x\varepsilon})^2} \left(\frac{\sigma_{x\varepsilon}}{d}\right)^2 \tag{18}$$

where d is the minimum halfwidth of the vacuum chamber in Adone. With d = 7 cm, τ_x = 174 msec and η = 2 m, we get:

$$\tau_{qx} \simeq 56 \text{ sec} . \tag{19}$$

4.3. - RF acceptance.

With similar arguments we can write the beam lifetime for energy oscillations, by assuming a gaussian energy spread distribution function, as

$$\tau_{q\varepsilon} = \tau_s \, e^{\left(\varepsilon_{RF}/\frac{\Delta\gamma}{\gamma}\right)^2} \left(\frac{\Delta\gamma/\gamma}{\varepsilon_{RF}}\right)^2 . \tag{20}$$

With τ_s = 87 msec we have

$$\tau_{q\varepsilon} \simeq 38 \text{ sec} \qquad \text{(1 RF cavity)}, \tag{21}$$

$$\tau_{q\varepsilon} \simeq 19 \text{ hours} \qquad \text{(2 RF cavities)} . \tag{22}$$

We observe that lifetimes under 4.2 and 4.3 are calculated by assuming gaussian e⁻ beam distributions. Actually, in a steady state laser operation, electrons should have (?) an harmonic oscillator energy distribution whose tails are more sharply cut than those of gaussian distributions. This should possibly lead to an increase of lifetimes.

5. - OPTICAL PARAMETERS.

According to eq. (6) the FEL gain is inversely proportional to the optical mode cross section $\bar{\Sigma}_L$ in the interaction region, provided the electron beam is fully contained within the laser beam ($\bar{\Sigma}_e < \bar{\Sigma}_L$).

The laser beam cross section $\bar{\Sigma}_L$ is given by

$$\bar{\Sigma}_L = \frac{1}{L_w} \int_{-L_w/2}^{L_w/2} \Sigma_L(y)\, dy = \frac{2\pi w_o^2}{L_w} \int_0^{L_w/2} \left[1 + \left(\frac{\lambda y}{\pi w_o^2}\right)^2\right] dy \tag{23}$$

where L_w is the lenght of the interaction region and w_o is the beam waist for a TEM_{oo} gaussian mode.

The optimum beam waist can be found by minimizing the mode cross section

$$\frac{d}{dw_o} \bar{\Sigma}_L = 0 , \tag{24}$$

which implies

$$w_o = \sqrt{\frac{L_w \lambda}{2\pi\sqrt{3}}} . \tag{25}$$

By substituting eq. (25) into eq. (23) we have:

$$\bar{\Sigma}_L = \frac{L_w \lambda}{\sqrt{3}} \quad . \tag{26}$$

For $\lambda = 5145$ Å (our experiment) the optimum beam waist becomes $w_o \approx 0.35$ mm.

5.1. - The amplification experiment.

A possible layout of the amplification experiment is sketched in Fig. 8a.

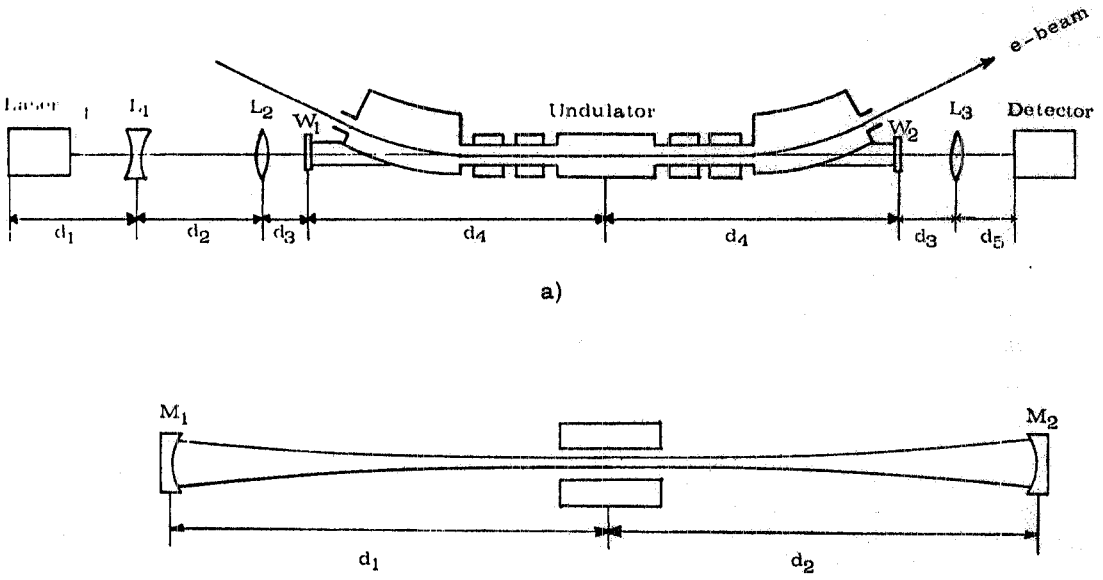

FIG. 8 - a) Schematic layout of the amplification experiment. b) Schematic layout of the oscillation experiment.

Here L_i are spherical lenses with focal lengths F_i and W_i are quartz windows. The "seed" laser to be used will be the Spectra-Physics SP 164-09 model operating in single line mode at 5145 Å. In order to have $w_o = 0.35$ mm at the undulator mid-point[14] distances and focal lengths can be choosen as follows:

$d_1 = 2.60$ m
$d_2 = 2.69$ m
$d_3 = 0.40$ m
$d_4 = 6.0$ m
$d_5 = 0.91$ m

$F_1 = -2.5$ m
$F_2 = 2.5$ m
$F_3 = 0.8$ m

5.2. - The oscillator experiment.

The optical cavity parameters must also be choosen so as to produce a waist $w_o = 0.35$ mm at the center of the interaction region for a wavelength $\lambda = 5154$ Å.

In Fig. 8b M_i are concave mirrors with curvature radii R_i. The FEL undulator can be inserted either in the Adone straight section no. 11 (as shown in Fig. 1) or in the diametrically op-

posite section (no. 5). In this last case it is not possible to have $d_1 = d_2$ because of existing obstructions on the floor (Synchrotron light channel PULS).

In Table V we show the optical cavity parameters calculated for the two possible insertions. W_i are the beam sizes on the mirrors and the corresponding Fresnel numbers $\mathcal{N} = a^2/d\lambda$ are calculated assuming the mirror size a is equal to the largest w_i.

TABLE V

d_1(m)	d_2(m)	w_o(mm)	w_1(mm)	w_2(mm)	R_1(m)	R_2(m)	$\mathcal{N}$	$(1 - \frac{d_1+d_2}{R_1})(1 - \frac{d_1+d_2}{R_2})$
8.75	8.75	0.35	4.14	4.14	8.81	8.81	2.2	0.973
8	9.5	0.35	3.76	4.46	8.07	9.56	2.2	0.971

In Figg. 9a and 9b we show the e^- beam and laser beam profiles along the interaction region in the radial and vertical plane respectively.

The e^- beam dimensions are plotted for two values of the betatron oscillation coupling factor $\chi^2 \approx 0.42$ (circular e-beam) and $\chi^2 \approx 0.01$, which corresponds to the minimum coupling experimentally obtained in Adone and gives an approximate flat beam.

Once the measured gain values will be available, it will be possible to work out the detailed project of the optical cavity and, in particular, to decide whether to build it completely "in vacuo" or not.

Acknowledgements.

We want to thank prof. C. Mencuccini and prof. R. Scrimaglio for constant encouragment and support, prof. S. Tazzari for many useful discussions, Dr. Eng. A. Cattoni for suggesting the feasibility and helping in the design of the short wavelength transverse undulator.

We also gratefully acknowledge help from LNF Accelerator and Technical Division Staffs, and secretary assistance done by Mrs. G. Possanza.

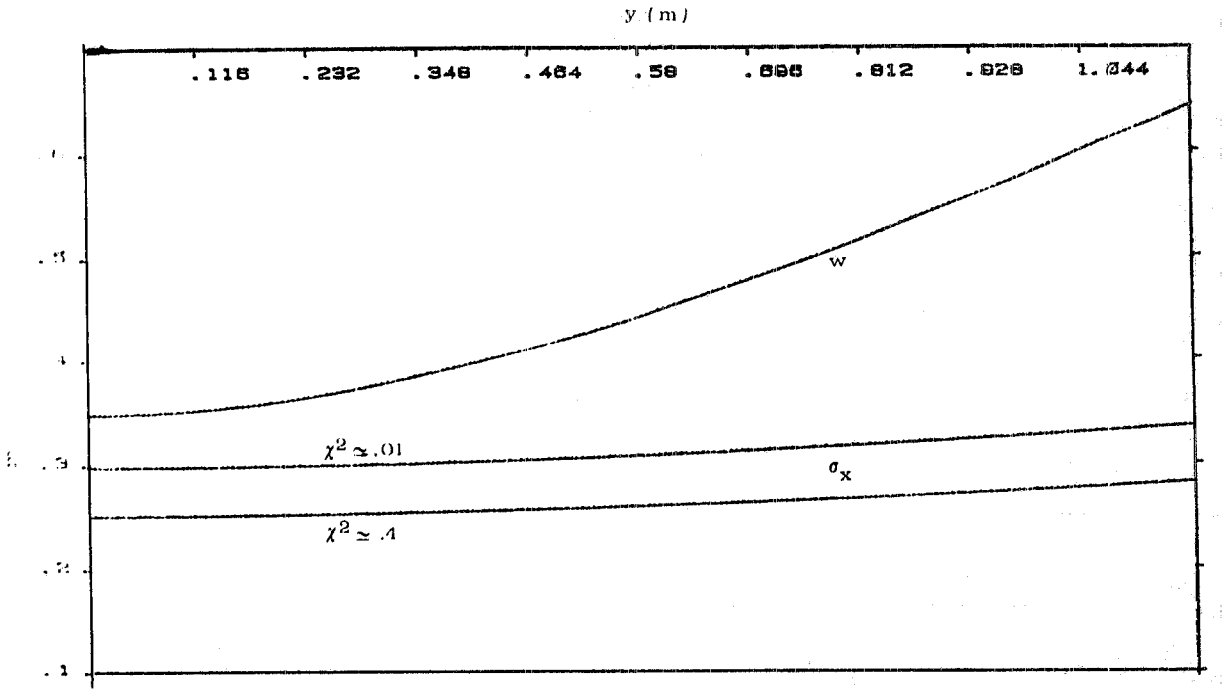

a)

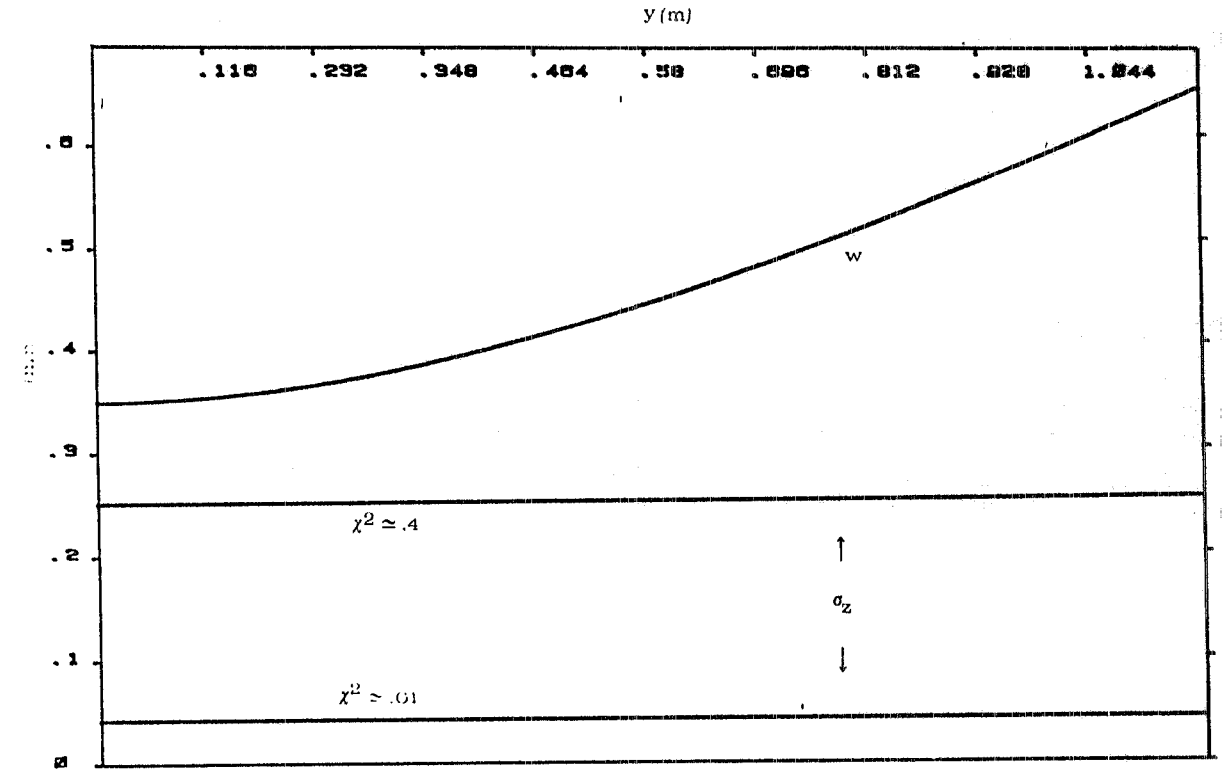

b)

FIG. 9 - Electron beam and laser beam profiles, along the interaction region. a) Radial plane, b) Vertical plane.

APPENDIX A - Fields and orbits in the FEL undulator.

a) Basic equations

Extensive runs of the CERN program MAGNET showed[5, 6] that the magnetic field in the gap (g = 4 cm) of the undulator (see Fig. 10)

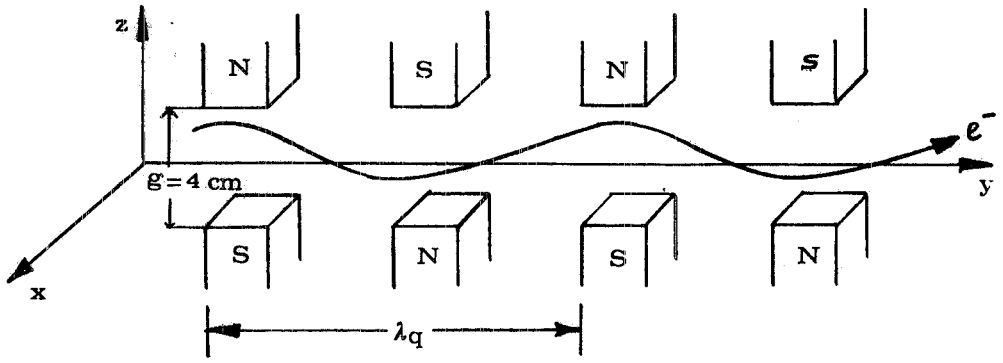

FIG. 10 - Schematics of the FEL undulator.

can be described by the following equations :

$$B_x = 0 , \qquad B_y = -B_o \sinh kz \sin ky , \qquad B_z = B_o \cosh kz \cos ky , \tag{A1}$$

with

$$k = \frac{2\pi}{\lambda_q} , \qquad \lambda_q = 11.6 \text{ cm} , \qquad B_o = 4459 \text{ G} . \tag{A2}$$

The equations of motion of the electron within this magnetic field[15] read (in C. G. S. -Gauss units and with $K_o = \frac{e B_o \lambda_q}{2\pi m_o c^2}$) :

$$\begin{aligned} \ddot{x} &= \frac{e}{m_o c \gamma} (\dot{y} B_z - \dot{z} B_y) = \frac{K_o c}{\gamma} \frac{d}{dt} \left[\cosh kz \sin ky\right] , \\ \ddot{y} &= - \frac{e}{m_o c \gamma} \dot{x} B_z = - kc \frac{K_o}{\gamma} \dot{x} \cosh kz \cos ky , \\ \ddot{z} &= \frac{e}{m_o c \gamma} \dot{x} B_y = - kc \frac{K_o}{\gamma} \dot{x} \sinh kz \sin ky . \end{aligned} \tag{A3}$$

Since, with our beam transverse dimensions we always have $kz \ll 1$, we can replace the hyperbolic functions by their first order series developments :

$$\sinh kz \approx kz , \qquad \cosh kz \approx 1 .$$

We then get :

$$\ddot{x} = \frac{K_o c}{\gamma} \frac{d}{dt} (\sin ky) , \qquad \ddot{y} = - kc \frac{K_o}{\gamma} \dot{x} \cos ky , \qquad \ddot{z} = - kc \frac{K_o}{\gamma} \dot{x} kz \sin ky . \tag{A4}$$

Integration of $\ddot{x}$ yields

$$\dot{x} - \dot{x}_o = \frac{K_o c}{\gamma} \int_0^t \frac{d}{dt} \sin (ky) = \frac{K_o c}{\gamma} \sin (ky) . \tag{A5}$$

Setting $\dot{x}_o = 0$ in (A5) we get from (A4) :

$$\ddot{y} = -(\frac{K_o}{\gamma})^2 k c^2 \sin ky \cos ky , \tag{A6}$$

$$\ddot{z} = -(\frac{K_o}{\gamma})^2 k^2 c^2 z \sin^2 ky . \tag{A7}$$

With the transformation

$$\frac{d}{dt} = \frac{d}{dy}\frac{dy}{dt} \tag{A8}$$

eq. (A6) can readily be integrated to yield

$$\dot{y}^2 - \dot{y}_o^2 = -c^2(\frac{K_o}{\gamma})^2 \sin^2 ky . \tag{A9}$$

By averaging the $\sin^2 ky$ term over one period of the undulator

$$\frac{1}{\lambda_q}\int_0^{\lambda_q} \sin^2 ky\, dy = \frac{1}{2} , \tag{A10}$$

we obtain from (A9) the RMS velocity along y (c units)

$$\beta^{*2} = \langle \dot{y}^2/c^2 \rangle = (\dot{y}_o/c)^2 - \frac{1}{2}(\frac{K_o}{\gamma})^2 = 1 - \frac{1}{\gamma^2}(1 + \frac{1}{2}K_o^2) , \tag{A11}$$

whence

$$\beta^* \cong 1 - \frac{1}{2\gamma^2}(1 + \frac{1}{2}K_o^2) . \tag{A12}$$

We can set, to all orders of approximation

$$y = \beta^* ct . \tag{A13}$$

b) Wavelength equation

The expression for resonance wavelength can be found by imposing that the slippage between E. M. wave and electron in travelling one undulator period λ_q be equal to one optical wavelength. Since the slippage $c\Delta\tau$ is given by:

$$c\Delta\tau = \lambda_q(\frac{1}{\beta^*} - 1), \tag{A14}$$

we get from (A12):

$$c\Delta\tau = \lambda = \lambda_q(\frac{1}{\beta^*} - 1) = \frac{\lambda_q}{2\gamma^2}(1 + \frac{1}{2}K_o^2) . \tag{A15}$$

Eq. (A15) agrees with eq. (1) since

$$K = \frac{1}{\sqrt{2}} K_o . \tag{A16}$$

It is easy to show that if the electron enters the undulator with an angle $\theta_e \neq 0$ with respect to y axis, then eq. (A15) must be replaced by eq. (B2) of Appendix B.

c) Transfer matrices

Eq. (A7), with positions (A8) and (A10) can now be written as ($\beta^* \simeq 1$) :

$$\frac{d^2 z}{dy^2} = - K_{eq}^2 z \tag{A17}$$

with the equivalent quadrupole strength given by

$$K_{eq} = \frac{K_o}{\gamma} \frac{2\pi}{\lambda_q} \frac{1}{\sqrt{2}} . \tag{A18}$$

The equation of motion (A17) implies[11] the following vertical transfer matrix for the undulator :

$$M_v = \begin{pmatrix} \cos(K_{eq} L_w) & \frac{1}{K_{eq}} \sin(K_{eq} L_w) \\ - K_{eq} \sin(K_{eq} L_w) & \cos(K_{eq} L_w) \end{pmatrix} \tag{A19}$$

where L_w is the undulator length. We notice that the undulator acts as a focussing Q-pole in the vertical plane.

By a similar procedure one can demonstrate that, on the horizontal plane the undulator acts as a straight section, i.e. its matrix is :

$$M_H = \begin{pmatrix} 1 & L_w \\ 0 & 1 \end{pmatrix} . \tag{A20}$$

The same matrices have been obtained by Bassetti et al.[16] with a calculation based on a rectangular model for the wiggler magnetic field.

APPENDIX B - Homogeneous and inhomogeneous broadening.

The homogeneous line broadening arises from the finite interaction time of the electron in the N-periods undulator, and is given by :

$$\left(\frac{\Delta\lambda}{\lambda}\right)_o = \frac{1}{2N} = 2.5\% . \tag{B1}$$

The inhomogeneous broadening is due to the finite dimensions, angular and energy spread of the e^- beam. The central wavelength of the radiation emitted by an electron travelling at an angle θ_e with respect to the undulator axis is given by :

$$\lambda = \frac{\lambda_q}{2\gamma^2} (1 + K^2 + (\gamma\theta_e)^2) . \tag{B2}$$

By differentiating this formula and folding with e^- beam gaussian distributions, we find the various contributions to the inhomogeneous spread :

$$\left(\frac{\Delta\lambda}{\lambda}\right)^i_\gamma = 2 \frac{\sigma_\gamma}{\gamma} = 2\sigma_p , \tag{B3}$$

$$\left(\frac{\Delta\lambda}{\lambda}\right)^i_{\theta_e} = \frac{\gamma^2}{1 + K^2} \sigma^2_{\theta_e} , \tag{B4}$$

$$\left(\frac{\Delta\lambda}{\lambda}\right)^{i}_{B_z} = \frac{2K^2}{1+K^2}\left(\frac{\Delta B_z}{B_z}\right) . \tag{B5}$$

The vertical field off the undulator midplane can be fairly well approximated (see also Appendix A) by:

$$B_z(y,z) = B_o \cos\left(\frac{2\pi}{\lambda_q} y\right) f(z) , \tag{B6}$$

where

$$f(z) = 1 + \alpha z^2 . \tag{B7}$$

According to our calculations[5, 6]:

$$\alpha \approx 1.4 \times 10^{-3}\ \text{mm}^{-2} . \tag{B8}$$

Eq. (B5) then becomes:

$$\left(\frac{\Delta\lambda}{\lambda}\right)^{i}_{B_z} = \frac{2K^2}{1+K^2}\ \alpha\sigma_z^2 . \tag{B9}$$

With the ring optics displayed in Figg. 3, 4, 9 we have ($\sigma_p = 2.3 \times 10^{-4}$) at the interaction region mid-point

	$\chi^2 = 0.01$	$\chi^2 = 0.42$
$\sigma_{\theta_x} = \frac{\sigma_x}{\beta_x}$	1.36×10^{-4}	1.14×10^{-4}
$\sigma_{\theta_z} = \frac{\sigma_z}{\beta_z}$	5.6×10^{-6}	4.7×10^{-5}
$\sigma_{\theta_e} = \sqrt{\sigma^2_{\theta_x} + \sigma^2_{\theta_z}}$	1.36×10^{-4}	1.23×10^{-4}

(B10)

therefore

$$\left(\frac{\Delta\lambda}{\lambda}\right)^{i}_{\gamma} \simeq 4.6 \times 10^{-4}$$

$$\left(\frac{\Delta\lambda}{\lambda}\right)^{i}_{\theta_e} \simeq 2.1 \times 10^{-3} \qquad \left(\frac{\Delta\lambda}{\lambda}\right)^{i}_{\text{Total}} = 2.16 \times 10^{-3} . \tag{B11}$$

$$\left(\frac{\Delta\lambda}{\lambda}\right)^{i}_{B_z} \simeq 1.6 \times 10^{-4}$$

We clearly see that the condition for homogeneous broadening is fulfilled.

Fig. 11a shows the results of a numerical calculation[19] of the homogeneous spectrum on axis (1st harmonic) together with the spectrum obtained by folding in the gaussian e-beam radial, angular and energy distributions.

We see that the two spectra have practically the same fractional linewidth which again confirms the inhomogeneous effects to be negligible.

For the sake of completeness we also show (Fig. 11b) the total spectrum integrated over a circular counter subtending a solid angle $\Delta\theta\Delta\varphi = 0.2 \times 10^{-3} \times 2\pi$ rad^2. This last information will be useful in the course of the alignment procedures.

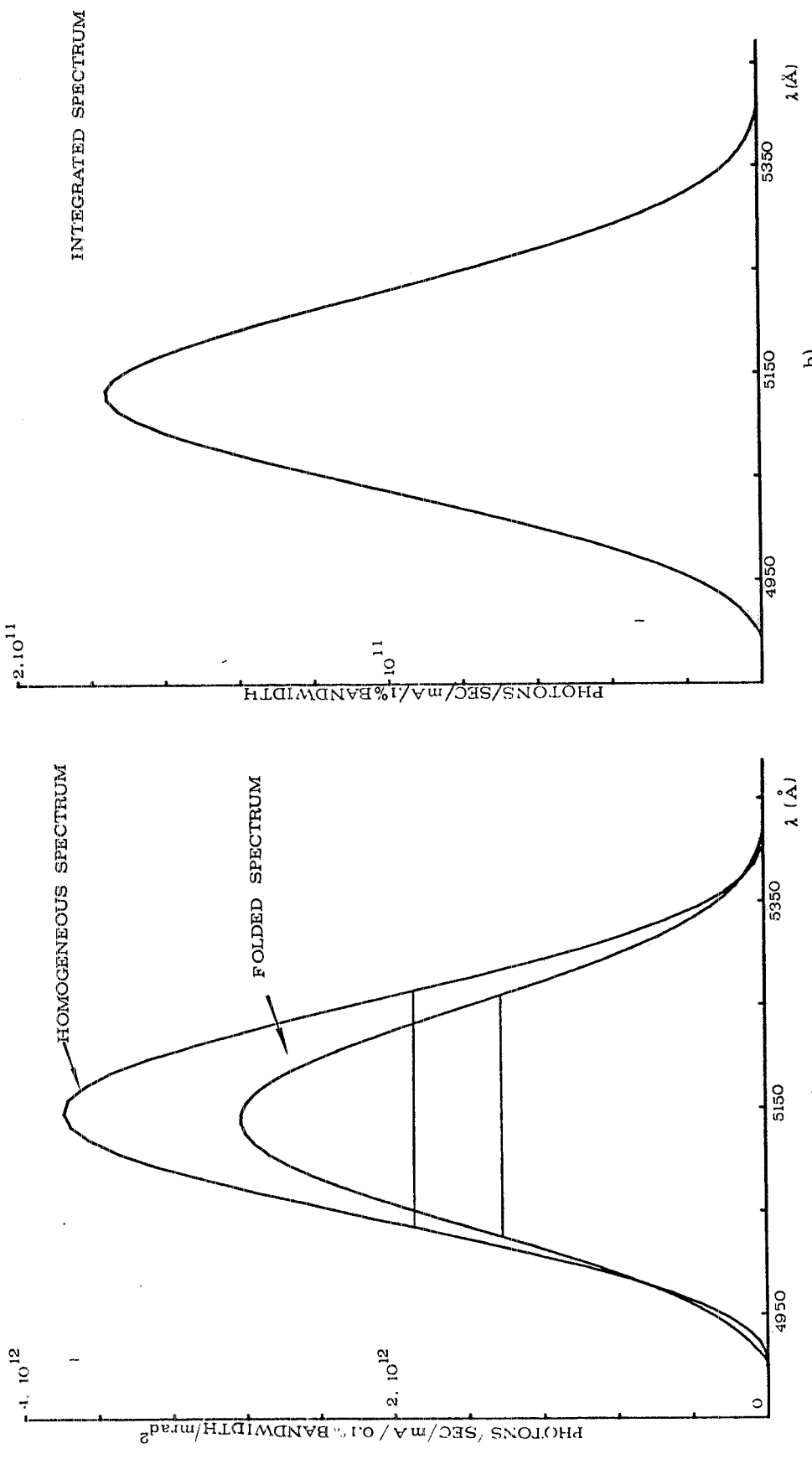

FIG. 11 - Spontaneous radiation spectrum. a) Homogeneous and folded spectrum for $\theta = 0$. b) Integrated spectrum over a counter acceptance $\Delta\varphi\Delta\theta = 2\pi \times 0.2 \times 10^{-3}$ rad^2.

APPENDIX C

We apply eq. (6) derived in reference (4) on the basis of Colson's theory[8] to the Madey's data (oscillator experiment) reported in ref. (17) :

$$\lambda = 3.41\ \mu m\ , \qquad \lambda_q = 3.23\ cm\ , \qquad K^2 = 0.52\ ,$$

$$N = 161\ , \qquad i_p = 0.66\ A\ , \qquad E = 43.5\ MeV.$$

Laser waist $w_o = 1.71$ mm (as calculated from mirrors' curvature radii $R_1 = R_2 = 7.5$ m and cavity length $d = 12.7$ m).

With the above parameters eq. (6) yields, for the homogeneously broadened small signal gain

$$g_o = 12.74\ \%$$

by taking for $\overline{\Sigma}_L$ expression (23). This value is to be compared with the quoted experimental value $g_{exp} \simeq 15\ \%$.

REFERENCES

(1) - L. R. Elias, W. M. Fairbank, J. M. J. Madey, H. A. Schwettman and T. I. Smith, Phys. Rev. Letters 36, 717 (1976).

(2) - D. A. G. Deacon, L. R. Elias, J. M. J. Madey, G. J. Ramian, H. A. Schwettman and T. I. Smith, Phys. Rev. Letters 38, 802 (1977).

(3) - C. Pellegrini, in "Wiggler Meeting", Frascati, June 29-30, 1978, ed. by A. Luccio, A. Reale and S. Stipcich (LNF, 1978).

(4) - C. Pellegrini, IEEE Trans. on Nuclear Sci., NS-26, 3791 (1979); C. Pellegrini, in "Report on FEL Workshop", Riva del Garda, June 4-6, 1979, ed. by G. Scoles.

(5) - R. Barbini, M. E. Biagini and G. Vignola, Sul campo magnetico dell'ondulatore per il FEL, Adone Internal Memo MA-44 (1979).

(6) - A. Cattoni, Progetto di massima di un ondulatore per il FEL, Adone Internal Memo MA-45 (1979); A. Cattoni e C. Sanelli, Calcolo di un ondulatore per Adone: minimo λ_q, Adone Internal Memo MA-46 (1979); B. Dulach, Ondulatore: calcolo delle deformazioni meccaniche, Adone Internal Memo IDT-16 (1979).

(7) - Groupe "Supraconducteurs", CEN-Saclay Report DPh/PE-STIPE SUPRA/78-35 (1978).

(8) - W. B. Colson, Phys. Letters 59A, 187 (1976); 64A, 190 (1977).

(9) - A. W. Chao and J. Gareyte, Scaling law for bunch lengthening in SPEAR II, Report SPEAR 197/PEP 224 (1976).

(10) - S. Tazzari, Scaling dell'allungamento anomalo, Adone Internal Memo T-93 (1978).

(11) - M. Sands, The physics of electron storage rings. An introduction, Report SLAC-121, UC-28(ACC) (1970).

(12) - H. Bruck, Accelerateur Circulaires de Particules (Presses Univ. de France, 1966), p. 268.

(13) - H. Bruck, ibidem, Chapter XXX and XXXI.

(14) - G. Giordano and E. Poldi Alai, Geometry of gaussian beams and laser cavities, Frascati Report LNF-79/4 (1979).

(15) - J. P. Blewett and R. Chasman, in "Workshop on Wiggler Magnets at SLAC", Stanford, March 1977, SSRP Report No. 77/05 (1977).

(16) - M. Bassetti, A. Cattoni, A. Luccio, M. Preger and S. Tazzari, A transverse wiggler magnet for Adone, Frascati Report LNF-77/26 (1977); M. Bassetti and S. Tazzari, in "Wiggler Meeting", Frascati, June 29-30, 1978, ed. by A. Luccio, A. Reale and S. Stipcich (LNF, 1978).

(17) - J. M. J. Madey and H. A. Schwettman, Final technical report to ERDA, Contracts : Ey 76-S-03-0326 PA 48 and PA 49.

(18) - F. H. Wang, Touschek lifetime at Adone and beam size, Adone Internal Memo T-113 (1979).

(19) - R. Barbini and G. Vignola, The LELA undulator as a source of synchrotron radiation, Adone Internal Memo G-32 (1979).